Viscoelastic Behavior of Degradable Polyolefins Aged in Soil

L. CONTAT-RODRIGO, A. RIBES-GREUS

Department of Applied Thermodynamics, ETSIIV, Universidad Politécnica de Valencia, Apartado 22012, 46071 Valencia, Spain

Received 13 September 1999; accepted 9 February 2000

ABSTRACT: Samples of polypropylene and a high density polyethylene/polypropylene blend filled with different biodegradable additives (rice starch/iron oxide mixture, Bioefect 72000 and Mater-Bi AF05H) have been subjected to an outdoor soil burial test for 21 months. Changes on the morphology of the samples have been studied by differential scanning calorimetry. The degradation process also has been analyzed in terms of the mechanical behavior of the polymers. The three characteristic relaxation zones α, β, and γ (in order of decreasing temperature) of the dynamic-mechanical relaxation spectra of the samples have been characterized according to the Fuoss–Kirkwood equation. When two relaxations were overlapped, a deconvolution method was applied. It has been observed that the degradation process affects just to a small extent the amorphous phase of the polymers. That the β relaxation is the most sensitive to the exposure time suggests that degradation starts in the crystalline–amorphous interface. However, the crystalline phase is also affected significantly by the degradation process. The mechanical results are in good agreement with the calorimetric measurements, proving that degradation takes place in two stages with different time scales depending on the additive used. © 2000 John Wiley & Sons, Inc. J Appl Polym Sci 78: 1707–1720, 2000

Key words: degradable polyolefins; soil burial test; dynamic-mechanical spectroscopy; differential scanning calorimetry

INTRODUCTION

Most of the synthetic plastics were designed to be resistant to environmental degradation. However, the awareness of the problems related to the uncontrolled growing of the volume of solid wastes has lead to an increasing interest in the development of degradable plastics. Up to half of the plastic production ends up as waste within two years since it is not used for long-term applications. The development of degradable polymers therefore offers a promising alternative for products that have a short life cycle or are impractical to recycle.

Polyolefins, one of the most important commodity plastics, are considered as not biodegradable polymers since they are not easily metabolized by microorganisms. Nevertheless, it is possible to enhance their biodegradability by simply incorporating additives that increase their oxidative degradation rate to the polymeric matrix in the form of a master batch.[1–6]

The estimation of the degradation rate of such degradable polyolefins is essential to predetermine their service life and thus to evaluate the viability of the use of these materials for a specific application. Polymer degradation is manifested by changes in its chemical and physical proper-

Correspondence to: A. Ribes-Greus.

Journal of Applied Polymer Science, Vol. 78, 1707–1720 (2000)

Table I Samples Composition

Sample	Polymeric Matrix	Additive
A	HDPE/PP (40/60% weight)	Rice starch/iron oxide (92/8% weight)
B	HDPE/PP (40/60% weight)	Bioefect 72000
C	HDPE/PP (40/60% weight)	Mater-Bi AF05H
D	PP	Bioefect 72000

ties. Analytical techniques such as Fourier transform infrared spectroscopy, size exclusion chromatography, gas chromatography—mass spectroscopy, chemiluminiscence have been used to analyze the changes on the chemical structure of the polymer during degradation. Identification of the compounds formed during the polymer degradation helps elucidate the mechanism of the degradation process.[7,8] On the other hand, physical changes are analyzed by means of other techniques such as differential scanning calorimetry (DSC) and tensile testing.

The objective of this work is the study of the dynamic mechanical relaxation spectrum and the morphological behavior of polyolefins filled with biodegradable additives aged in soil, in order to analyze and characterize their degradation process.

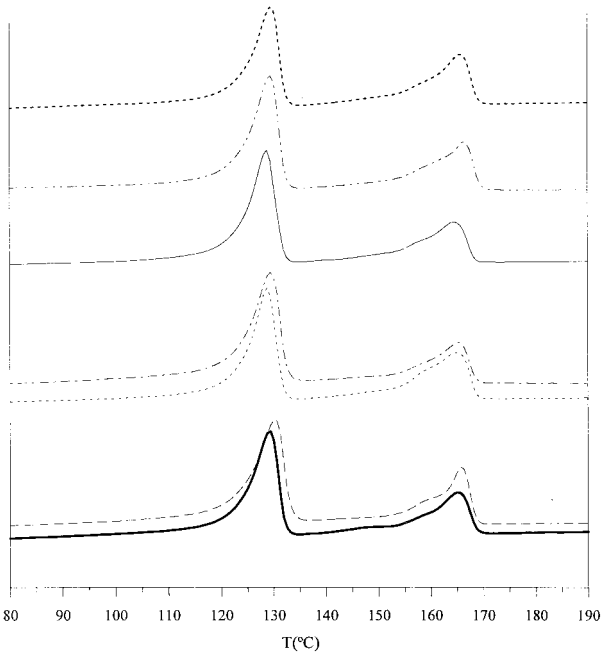

Figure 1 DSC thermograms of sample C after different exposure times: (–) undegraded; (- - -) 3 months; (· · ·) 6 months; (– · – · –) 9 months; (—) 12 months; (– ·· – ·· –) 15 months; (– – –) 21 months.

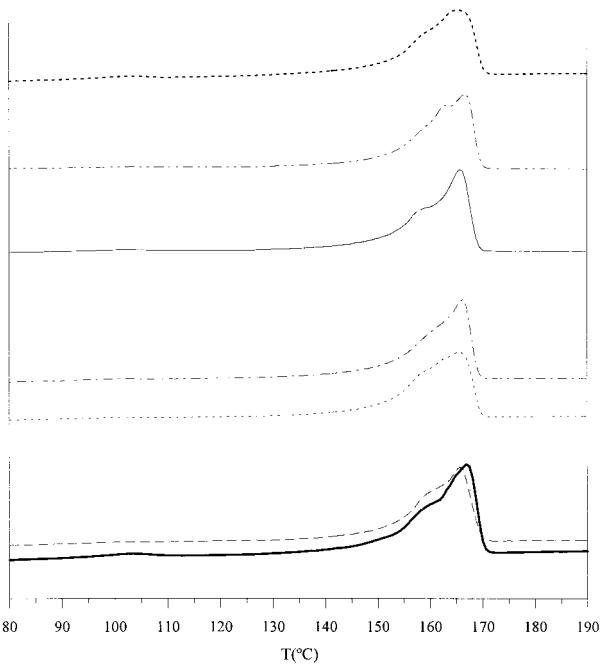

Figure 2 DSC thermograms of sample D after different exposure times: (–) undegraded; (- - -) 3 months; (· · ·) 6 months; (– · – · –) 9 months; (—) 12 months; (– ·· – ·· –) 15 months; (– – –) 21 months.

EXPERIMENTAL

Materials

High density polyethylene-5218 (HDPE) supplied by British Petroleum (Spain) and Polypropylene 1148-TC (PP) supplied by BASF (Germany) were used.

Rice granular starch, commercial iron oxide, Bioefect 72000 from Proquimaq Color, S.L. (Spain), and Mater-Bi AF05H from Novamont North America were used as additives.

Samples

Four kinds of samples labeled A–D were prepared. Their composition is detailed in Table I. Samples A–C have the same polymeric matrix made up of a 40/60% by weight HDPE/PP blend. The polymeric matrix of sample D is formed only by PP. All the samples contain 10% by weight of a different biodegradable additive: sample A contains a 92/8% by weight rice granular starch/iron

Table II Physical Characterization of Samples Aged in Soil for Different Exposure Times: Total Crystalline Content *X*, and Melting Temperatures[a]

Degradation Time (months)	T_1 (°C)	$(H_a - H_c)_1$ (J/g)	X_1	T_2 (°C)	$(H_a - H_c)_2$ (J/g)	X_2
Sample A						
0	128.9	56.0	0.19	165.5	53.4	0.26
3	128.8	84.1	0.29	165.2	41.6	0.20
6	129.2	79.1	0.27	166.2	46.0	0.22
9	130.0	93.8	0.32	165.0	38.2	0.18
12	128.7	71.0	0.24	165.9	49.4	0.24
15	128.9	62.3	0.21	166.4	53.7	0.26
21	128.6	56.5	0.19	166.0	54.5	0.26
Sample B						
0	129.7	82.2	0.28	166.1	41.8	0.20
3	128.9	87.4	0.30	166.2	40.0	0.19
6	128.5	94.8	0.32	165.4	38.2	0.18
9	128.8	87.1	0.30	165.1	39.9	0.19
12	128.8	94.2	0.32	164.8	37.1	0.18
15	129.5	91.0	0.31	165.5	39.8	0.19
21	128.7	85.2	0.29	166.0	39.2	0.19
Sample C						
0	129.2	78.7	0.27	165.1	35.7	0.17
3	130.2	78.8	0.27	165.8	38.2	0.18
6	128.7	78.8	0.27	164.9	44.0	0.21
9	129.4	89.9	0.31	165.3	33.3	0.16
12	128.6	82.9	0.28	164.4	37.1	0.18
15	129.3	88.0	0.30	166.4	41.1	0.20
21	129.6	80.6	0.28	165.7	42.8	0.20
Sample D						
0	—	—	—	166.9	98.6	0.47
3	—	—	—	165.7	107.1	0.51
6	—	—	—	165.5	102.6	0.49
9	—	—	—	166.1	109.9	0.53
12	—	—	—	165.8	107.7	0.52
15	—	—	—	166.7	103.5	0.50
21	—	—	—	165.3	101.2	0.48

[a] 1 and 2 indicate the values assigned to HDPE and PP, respectively.

oxide mixture, sample B and D contain Bioefect 72000, and sample C contains Mater-Bi AF05H. Samples have been processed by injection as seedboxes.

Soil Burial Test

Samples were subjected to an outdoor soil burial test in Ayora (Valencia, Spain) for 21 months. Samples were removed after different periods of time: 0, 3, 6, 9, 12, 15, and 21 months. After removal, they were carefully washed with a soap solution in order to stop the biodegradation process and dried with a piece of paper before being analyzed. The soil where samples were buried has a pH of 6.75 (measured in water).

DSC Measurements

The morphology of the samples was analyzed by DSC. Both the crystalline content and the melting temperature were measured with a Perkin Elmer DSC-4 calorimeter, previously calibrated with indium. A total of 5–6 mg of samples were weighed out in a standard aluminum pan. The sealed pans were scanned at a heating rate of 10°C/min from 0 to 200°C under nitrogen atmosphere.

Dynamic Mechanical Measurements

The viscoelastic properties were determined by means of a Polymer Laboratories, Ltd., Dynamic Mechanical Thermal Analyzer, Mark II DMTA,

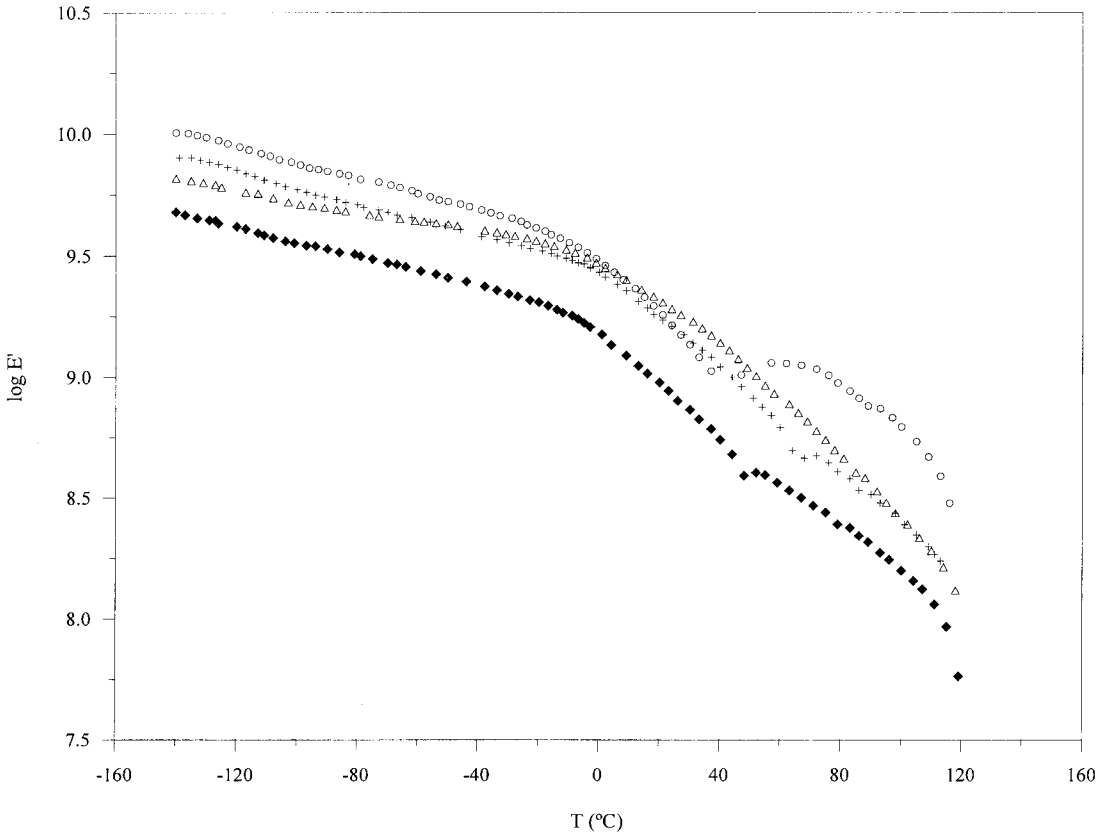

Figure 3 Plot of logE' versus temperature for sample B at 1 Hz of frequency for different degradation times: (♦) undegraded; (△) 6 months; (○) 12 months; (+) 21 months.

with deformation applied in the cantilever flexure double-clamping mode. The storage modulus E' and the loss tangent, tan δ were measured from −140 to 160°C at the frequencies of 0.3, 1, 3, 10, and 30 Hz with a heating rate of 1 °C/min.

RESULTS AND DISCUSSION

In order to analyze the changes on the morphology of the samples, DSC thermograms have been carried out for samples aged for different periods of time. Samples A–C have similar thermograms with two endothermic peaks, proving the incompatibility of the HDPE/PP blend.[9,10] Figure 1 shows as example the DSC thermograms of sample C after different exposure times. The first endothermic peak has been assigned to HDPE and the second one to PP. The thermogram of sample D displays just a single endothermic peak corresponding to PP, as shown in Figure 2. The peaks width of both endotherms indicates a wide lamellar sizes distribution. It is also observed that the peaks shape changes as the degradation time increases, especially that of the PP endotherm. This fact reveals that a transformation in the lamellar sizes distribution occurs due to the degradation process, especially in the PP phase. This result is in agreement with the idea that PP is much more susceptible to oxidation than polyethylene due to its methyl branches all along the backbone chain.[11] In the branch points, there is a hydrogen attached to a tertiary carbon that is more labile than the hydrogens of the methyl groups of the backbone chain. These labile hydrogens are thus more likely sites for the initiation of the oxidation process.

On the other hand, as HDPE and PP formed incompatible blends, two successive scans have also been performed in order to remove the processing effects. The first scan was carried out from 0 to 200°C at a heating rate of 10°C/min. After 10 min at 200°C, samples were cooled until 0°C at a cooling rate of 20°C/min. Finally, a sec-

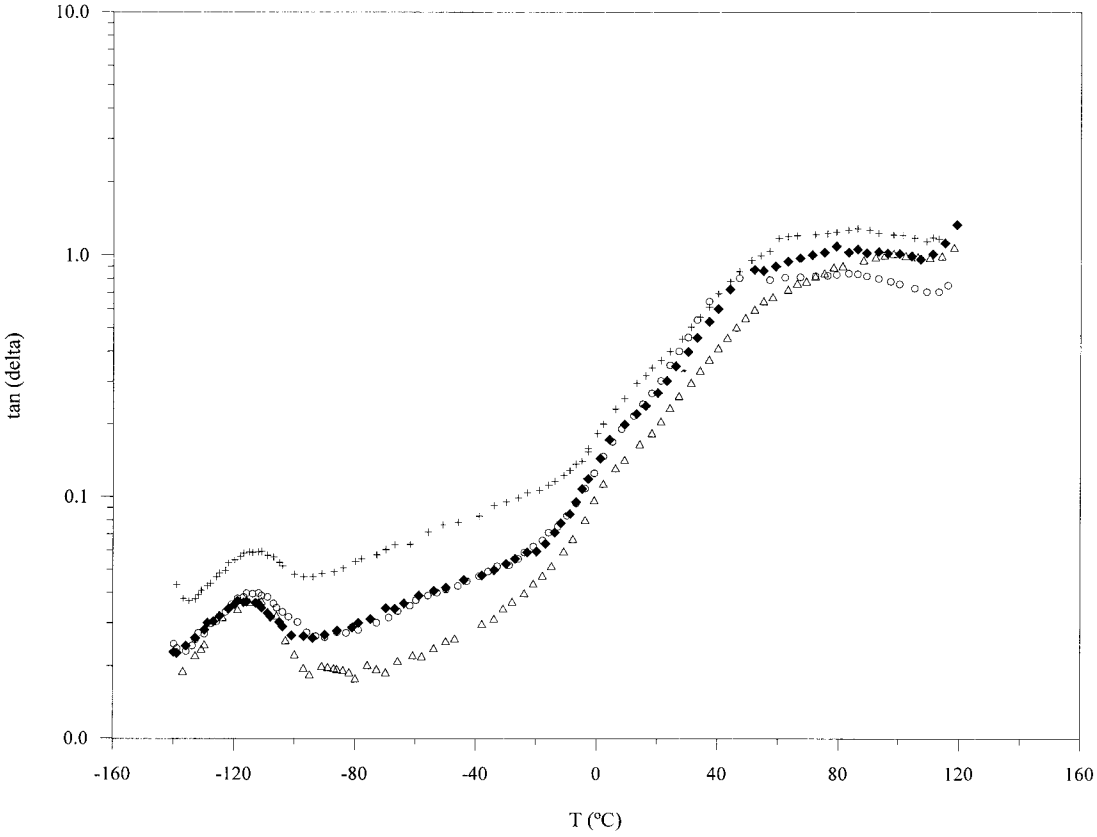

Figure 4 Plot of tan δ versus temperature of sample B at 1 Hz of frequency for different degradation times: (♦) undegraded; (△) 6 months; (○) 12 months; (+) 21 months.

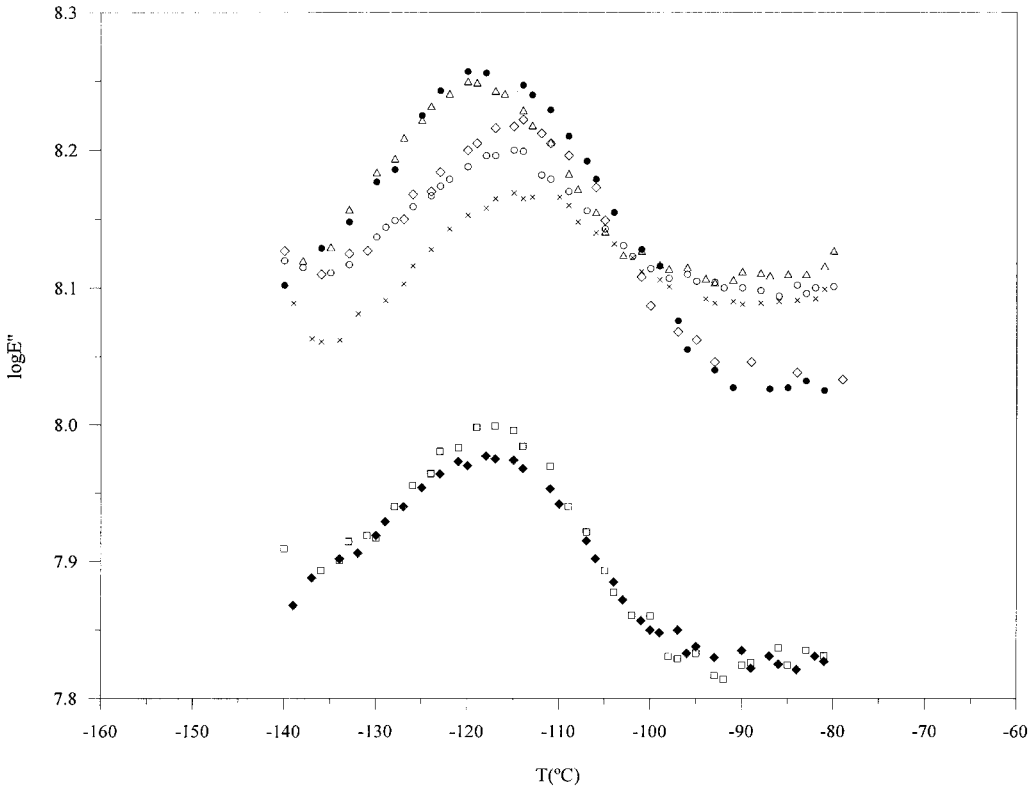

Figure 5 The γ relaxation zone of sample A at 1 HZ of frequency after different exposure times: (♦) undegraded; (□) 3 months; (△) 6 months; (●) 9 months; (◇) 12 months; (X) 15 months; (○) 21 months.

Table III Characterization of the γ Relaxation at 1 Hz of Frequency: Temperature of the Maximum of the Loss Modulus, T_m, Fuos–Kirkwood m Parameter, and Apparent Activation Energy E_a

Degradation Time (months)	T_m (°C)	m	E_a (kcal/mol)
Sample A			
0	−118.4	0.102	23.67
3	−118.4	0.111	24.57
6	−119.2	0.107	24.42
9	−118.1	0.108	22.96
12	−115.5	0.123	21.99
15	−114.4	0.080	24.33
21	−116.5	0.086	26.06
Sample B			
0	−119.9	0.095	25.92
3	−121.1	0.098	22.84
6	−119.9	0.105	26.63
9	−122.8	0.120	22.34
12	−118.9	0.116	19.25
15	−117.3	0.109	22.26
21	−118.7	0.103	21.22
Sample C			
0	−119.7	0.097	26.78
3	−117.2	0.108	23.54
6	−114.9	0.147	19.24
9	−117.8	0.110	20.52
12	−116.4	0.095	24.33
15	−115.0	0.108	22.00
21	−117.2	0.120	20.00

ond scan was carried out in the same conditions as the first one. The thermograms obtained from the second scan do not display the irregular peak shape as did the thermograms of the first scan. However, the crystallinity determined from the thermograms was found to be similar to that calculated when just a single scan was performed. These results show that the changes on the crystalline content and the lamellar sizes distribution are due to the degradation process and not to the samples processing.

The melting temperatures and the crystalline content have been determined for each sample (Table II). The melting temperatures have been directly obtained from the thermograms. It has been found a melting temperature of about 129°C for HDPE and around 166°C for PP, regardless of the additive used and the exposure time.

The crystalline content (X) of each homopolymer has been calculated for each sample according

$$X = \frac{(H_a - H_c)}{H_m} \quad (1)$$

where H_a and H_c are the enthalpies in the melt state and the crystalline state, respectively. Their difference is directly obtained form the thermogram. H_m is the change of the melting enthalpy of a perfect crystal of infinite size. For PE, H_m = 70 cal/g ≈ 293 J/g and for PP, H_m = 50 cal/g ≈209 J/g.[12]

The crystalline content of the samples aged in soil for different periods of time tends to change slightly although no regular evolution appears. These differences are however significant, since they are greater than the deviation between parallel runs within the same series. The changes in the crystalline content follow two stages. During the first stage, the crystalline content tends to increase. However, after 9 or 12 months of exposure (depending on each sample), a second stage begins during which the crystallinity tends to decrease. These results confirm the trend observed for the crystalline content of samples aged for 1 year shown by these authors in a previous work.[13] They also indicate that a degradation process is taking place as an increase in the crystallinity is considered as a degradation sign.[11] The reaction with a small amount of oxygen can produce the limited scission of the molecules of the crystalline–amorphous interface, so the crystallization can occur more rapidly.

Besides the analysis of the morphological changes, the degradation process has also been studied by means of the characterization of the mechanical behavior of the polymers. For this purpose, the complete relaxation spectrum of all the samples has been obtained.

The relaxation spectra of the samples exhibit three clearly distinguished relaxation zones α, β, and γ in order of decreasing temperature, although this latter relaxation just appears as a weak shoulder in the relaxation spectra of sample D as its polymeric matrix only contains PP. These results are in good agreement with the relaxation spectra predicted in the literature for HDPE/PP blends and pure PP.[14]

Work by Popli et al.,[15] as well as by ourselves,[16] have established that the α relaxation can be attributed to movements of molecular chains that occur in the crystalline zone. The β relaxation may result from motions taking place at the crystalline–amorphous interface. The γ relaxation can be associated to molecular chain movements in the amorphous phase of polyethylene.

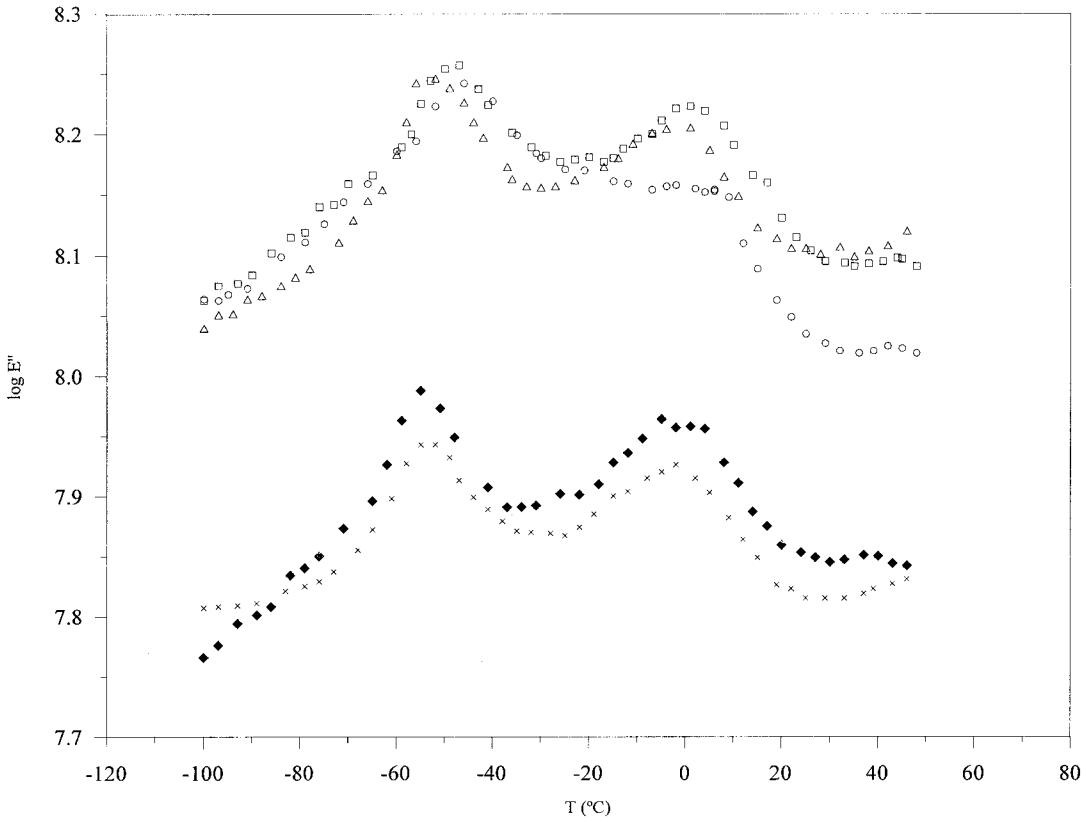

Figure 6 The β and α relaxation zones of sample D at 1 Hz of frequency after different exposure times: (♦) undegraded; (×) 3 months; (△) 6 months; (□) 12 months; (○) 21 months.

Figures 3 and 4 show as example respectively the relaxation spectrum in terms of the storage modulus (E') and the loss tangent (tan δ) versus temperature at the frequency of 1 Hz for sample B aged in soil for different periods of time. It can be noted from these figures, and from those of the other samples, that the degradation process affects basically E'. The storage modulus exhibits an initial increase, and although it tends to decrease slowly afterward, its values remain higher than that of the undegraded sample even after 21 months of exposure. This means that due to the degradation process the material becomes more brittle.

In this work, the mechanical properties of the samples have been analyzed with a Polymer Laboratories, Ltd., DMTA that measures the values of the storage modulus (E') and the loss tangent (tan δ). The values of the loss modulus (E'') are calculated from these two parameters, since tan δ is defined as the quotient between both moduli (tan $\delta = E''/E'$). E'' is thus estimated according to the relationship: $E'' = \tan \delta \times E'$.

As explained above, the obtained results show that E' is more modified than tan δ by the degradation process. For that reason, the analysis of the mechanical behavior is going to be carried out in terms of E'', which displays in a more obvious way the changes due to the degradation process.

Table IV Characterization of the β Relaxation of Samples D and C at 1 Hz of Frequency: Temperature of the Maximum of the Loss Modulus T_m, Fuos–Kirkwood m Parameter, and Apparent Activation Energy E_a

Degradation Time (months)	T_m (°C)	m	E_a (kcal/mol)
Sample D			
0	−56.2	0.095	66.47
3	−53.9	0.128	42.78
6	−54.2	0.142	55.13
9	−55.0	0.159	45.72
12	−50.8	0.118	51.47
15	−51.2	0.130	48.42
21	−48.0	0.096	51.31
Sample C			
15	−48.2	0.041	62.60
21	−37.3	0.032	69.81

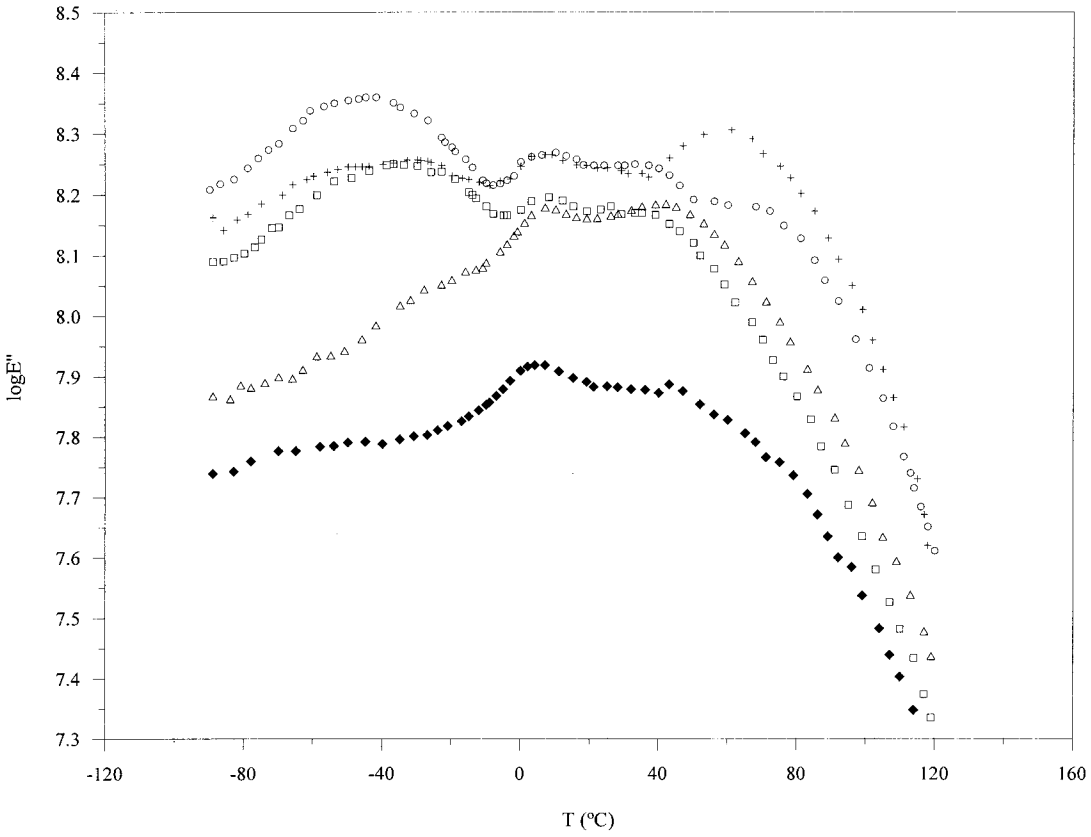

Figure 7 The β and α relaxation zones of sample C at 1 Hz of frequency after different exposure times: (♦) undegraded; (△) 6 months; (+) 12 months; (○) 15 months; (□) 21 months.

Each one of the relaxation zones has been characterized in order to analyze in more detail the mechanical behavior of the samples. The maximum of the loss modulus $E_{max''}$ the m parameter, and the temperature of the maximum of the loss modulus T_m have been obtained for each relaxation fitting its data to the Fuoss–Kirkwood equation:

$$E' = \frac{E'_{max}}{\cosh\left[m\frac{E_a}{R}\left(\frac{1}{T} - \frac{1}{T_m}\right)\right]} \qquad (2)$$

The apparent activation energy E_a of each relaxation has been calculated by adjusting the dependence of the mean relaxation times on the temperature to the Arrhenius equation:

$$\ln f_m = \ln f_0 + \exp(E_a/RT_m) \qquad (3)$$

where T_m and f_m are, respectively, the temperature and the frequency of the maximum of the loss modulus.

Figure 5 shows the γ relaxation of sample A in terms of log E'' as a function of temperature at 1 Hz of frequency. It is observed for all the samples that the maximum values of E'' increase gradually as the exposure time increases and finally tend to slightly decrease. It is also noted that T_m shifts to higher temperatures as the degradation time increases. The values of T_m, the Fuoss–Kirkwood m parameter and the apparent activation energy of this relaxation for samples A–C are listed in Table III. These parameters have not been calculated for sample D as it just exhibits a minor γ relaxation. Only slight variations of the Fuoss–Kirkwood m parameter and of the activation energies of the γ relaxation are observed. From these results, it can be concluded that the degradation process affects just to a small extent the amorphous phase of the polymers.

The β relaxation zone of polyolefins is located between −80 and −20°C. The characterization of this relaxation zone is more delicate since normally the β relaxation appears overlapped to the α one, as shown in Figure 6. In cases where there are two overlapped relaxations in a spectrum, it is

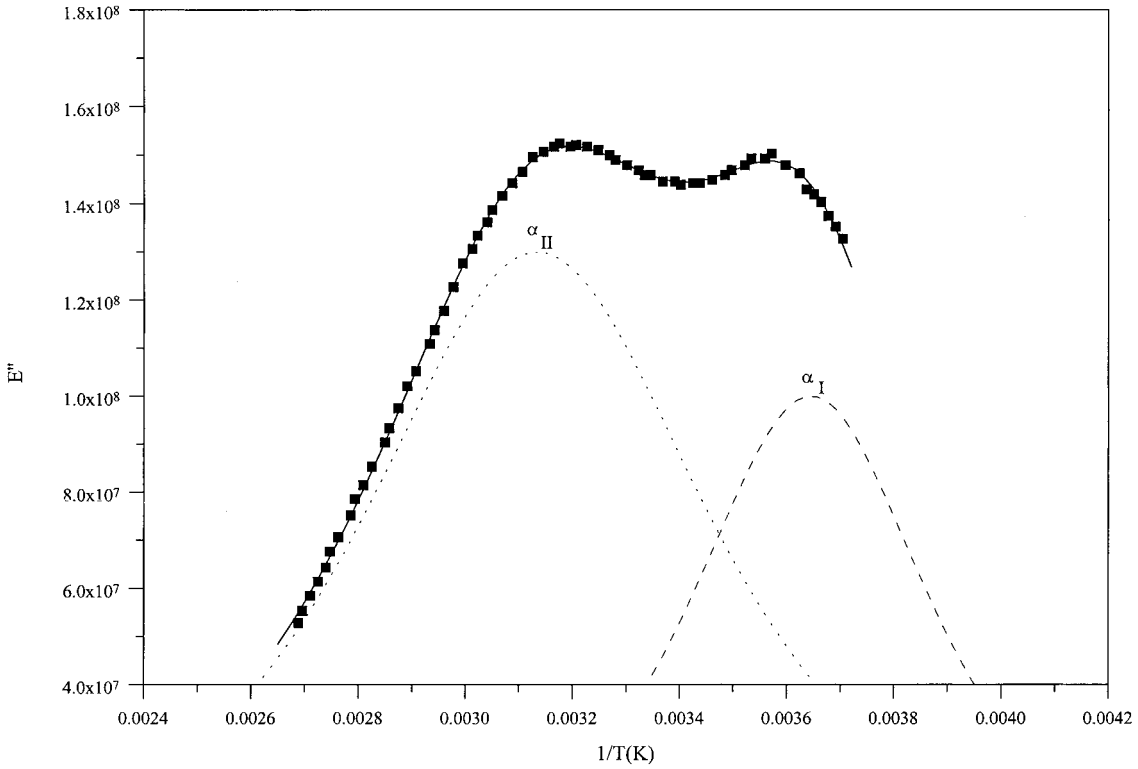

Figure 8 Deconvolution in terms of E'' of the α_I and α_{II} relaxations at 1 Hz of frequency for sample C in soil for 6 months: (■) experimental data; (—) values of E'' calculated by applying the deconvolution method together with the Fuoss–Kirkwood equation; (– – –) contribution of the α_I relaxation; (·····) contribution of the α_{II} relaxation.

supposed that the experimental data are the addition of these two relaxations. Thus the method used in the dynamic-mechanical spectra for the deconvolution of overlapped peaks considers that the measured value of E' is equivalent to $E'' = E''_I + E''_{II}$.[17]

Following this method, together with the Fuoss–Kirkwood equation, the β relaxation has been characterized for sample D. The other samples just display a minor β relaxation. Table IV summarizes the obtained results for sample D at 1 Hz of frequency after the deconvolution of the β and α relaxations. It can be observed that T_m shifts to higher temperatures as the exposure time increases. The Fuoss–Kirkwood m parameter has a maximum value at 9 months and afterward it tends to decrease. An irregular decrease in the activation energy is also observed. The changes in the m parameter and the decrease of E_a reveal that a certain reorganization of the molecular chains of the crystalline–amorphous interface has taken place so that their motions tend to be less hindered.

An inspection of the mechanical spectra of all the samples as a function of the aging time in soil demonstrates that the β relaxation zone is the most sensitive to the degradation process. Figure 7 shows that the β relaxation of sample C (located from −80 to −20°C) clearly increases its height as the exposure time increases. Depending on the additive used, this effect is more or less marked. As sample C is the one that exhibits this effect more significantly, it has been calculated the apparent activation energy of its β relaxation for 15 and 21 months of exposure, when the peak is more prominent (Table IV). Estimated values of about 60 kcal/mol has been found, similar to the ones obtained by these authors for high-density polyethylenes irradiated at low doses (2 and 20 Mrad).[18]

These results are in agreement with the idea that oxygen is usually insoluble in the crystalline regions of polyolefins.[19,20] Oxidation, and consequently the biodegradation process, will therefore be confined in the first stages in the chains between the crystallites that form the crystalline–

Table V Characterization of the α_I and α_{II} Relaxations at 1 Hz of Frequency: Temperature of the Maximum of the Loss Modulus T_m, Fuos–Kirkwood m Parameter and Apparent Activation Energy E_a

Degradation Time (months)	α_I Relaxation			α_{II} Relaxation		
	T_{mI} (°C)	m_I	E_{aI} (Kcal/mol)	T_{mII} (°C)	m_{II}	E_{aII} (kcal/mol)
Sample A						
0	−3.9	0.064	121.82	45.2	0.133	51.36
3	−5.7	0.098	85.96	38.9	0.193	30.31
6	2.0	0.068	126.58	48.1	0.117	52.21
9	−1.0	0.087	102.15	47.5	0.158	34.53
12	1.3	0.109	117.03	47.8	0.128	42.87
15	−1.0	0.078	99.31	52.0	0.115	52.03
21	−0.7	0.086	98.05	50.4	0.085	85.14
Sample B						
0	−0.6	0.093	127.11	41.5	0.143	36.53
3	−1.5	0.080	121.88	43.5	0.163	27.52
6	0.0	0.105	100.89	43.4	0.160	40.98
9	0.3	0.076	135.58	45.5	0.127	41.53
12	0.3	0.079	110.98	47.3	0.141	46.60
15	1.3	0.063	145.45	49.5	0.084	76.89
21	1.3	0.111	89.19	42.6	0.093	70.21
Sample C						
0	−1.1	0.075	115.80	49.9	0.134	41.39
3	4.1	0.163	87.67	40.9	0.176	38.19
6	1.4	0.084	120.80	46.2	0.147	47.91
9	−1.5	0.043	129.61	54.8	0.095	88.10
12	−0.2	0.067	137.30	44.5	0.146	42.85
15	−2.5	0.078	90.95	50.4	0.124	55.56
21	1.3	0.102	111.28	40.3	0.137	49.26
Sample D						
0	−0.7	0.042	138.78	49.8	0.158	30.33
3	2.0	0.049	119.02	56.8	0.096	58.41
6	1.3	0.036	173.47	56.1	0.102	53.04
9	5.9	0.051	83.10	53.3	0.125	40.55
12	5.2	0.043	139.70	53.6	0.147	35.95
15	6.7	0.039	180.51	61.0	0.138	37.05
21	7.3	0.051	155.40	47.2	0.148	33.28

amorphous interface. The development of a more prominent β relaxation could explain the displacement of the temperature of the maximum of the loss modulus T_m observed before for the γ relaxation.

The α relaxation zone of the samples studied display two overlapped relaxations called α_I and α_{II} in order of increasing temperature. The α_I relaxation appears as a small peak centered at about 0°C, whereas the α_{II} relaxation is a wide shoulder located around 45–50°C, as shown in Figure 7. The characterization of both relaxations has been performed according to the deconvolution method described above. Figure 8 shows as example the deconvolution of the α_I and α_{II} relaxation at 1 Hz of frequency for sample C aged in soil for 6 months. Table V displays the values of T_m, m, and E_a calculated for all the samples as a function of the degradation time. It is noted that the temperature of the maximum of the loss modulus, T_m of both the α_I and α_{II} relaxations also shifts to higher values as the exposure time increases, as it occurred for the γ and β relaxations. So it can be concluded that the degradation process produces a general shift of the mechanical spectrum of the samples toward higher temperatures.

Concerning the Fuoss–Kikwood m parameter, higher values were found for the α_{II} relaxation as expected, since this parameter is an indicative of the relaxation width.

In Figures 9–12 the apparent activation energies estimated for these two relaxations have

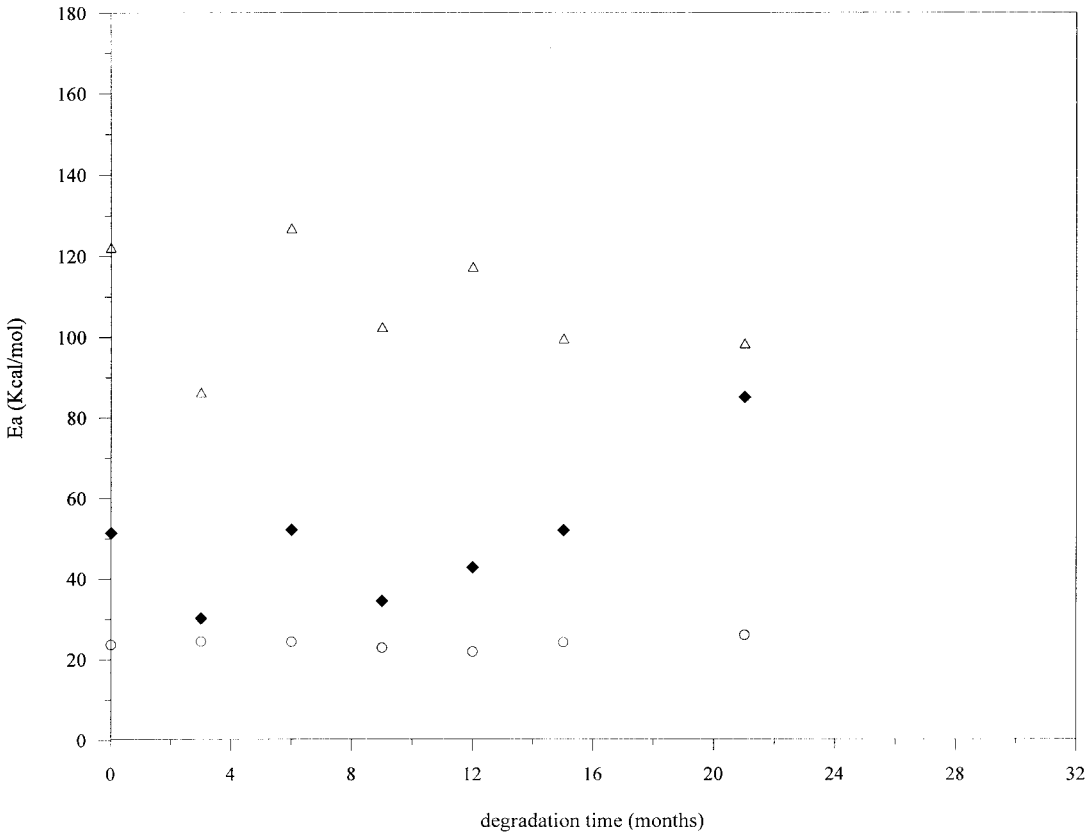

Figure 9 Apparent activation energies E_a of the (○) γ, (△) α_I, and (◆) α_{II} relaxations of sample A as a function of the degradation time.

been plotted together with those of the other characterized relaxations for each sample as a function of the degradation time. These figures show that the activation energies of the α relaxations are the ones that change the most during the degradation process. This means that the crystalline phase is considerably affected by degradation. Changes are specially marked for the α_I relaxation. This is consistent with the idea that the position of the different α relaxations in the temperature axis is dependent on the crystallites thickness.[16] This would indicate that the α_I relaxation is associated with motions of molecular chains of thinner crystallites than that involved in the α_{II} relaxation. Thinner crystallites are thus more affected by the degradation process than the thicker ones.

It is also noted from these figures that although the evolution of *Ea* of both α relaxations is quite irregular, the apparent activation energy of the α_I relaxation tends to decrease, whereas that of the α_{II} relaxation tends to increase. This phenomenon has a different time scale for each sample.

On the other hand, a close inspection of the mechanical spectra of the samples reveal that the height of the α_{II} relaxation initially increases, but after a period of 9 or 12 months (depending on each sample), it decreases. This tendency can be observed in Figure 6 for sample C. As stated by others,[16] the height of the α relaxation is associated to the crystalline content. Assuming this, the changes produced in the α relaxation zone can be correlated to the calorimetric results. In fact, the observed evolution of the α_{II} relaxation is in good agreement with the thermograms discussed before. The mechanical results confirm therefore the development of the degradation process in two stages. In a first stage, when the crystalline content increases and the lamellar sizes distribution changes, the α_{II} relaxation becomes higher. After 9 or 12 months of aging in soil (depending on each sample), when the crystalline content starts to decrease and the lamellar sizes exhibit a broad distribution, the height of the α_{II} relaxation diminishes.

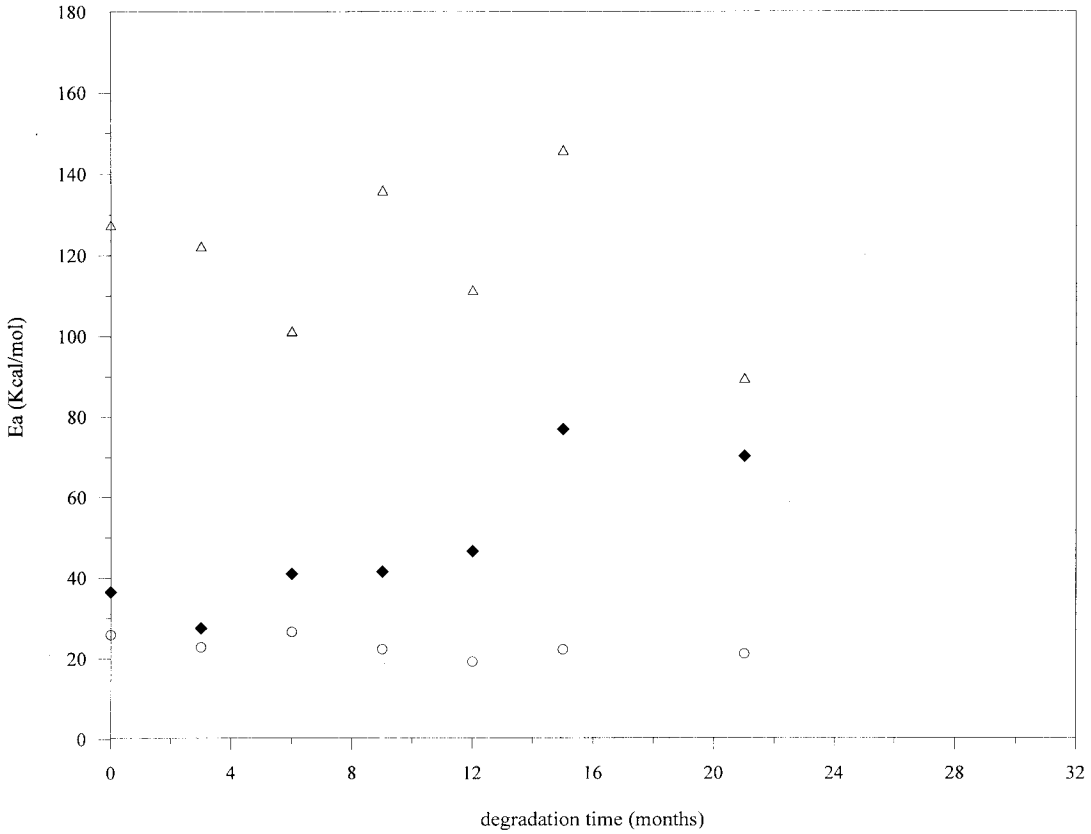

Figure 10 Apparent activation energies E_a of the (○) γ, (△) α_I, and (◆) α_{II} relaxations of sample B as a function of the degradation time.

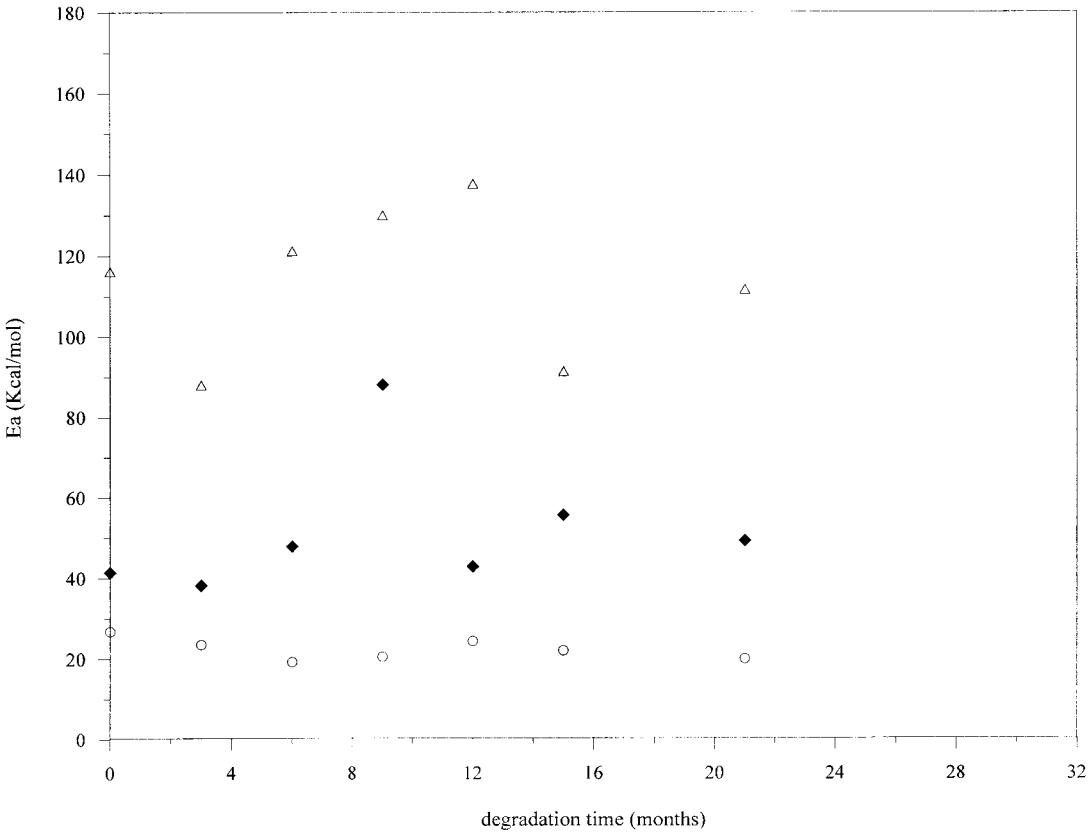

Figure 11 Apparent activation energies E_a of the (○) γ, (△) α_I, and (◆) α_{II} relaxations of sample C as a function of the degradation time.

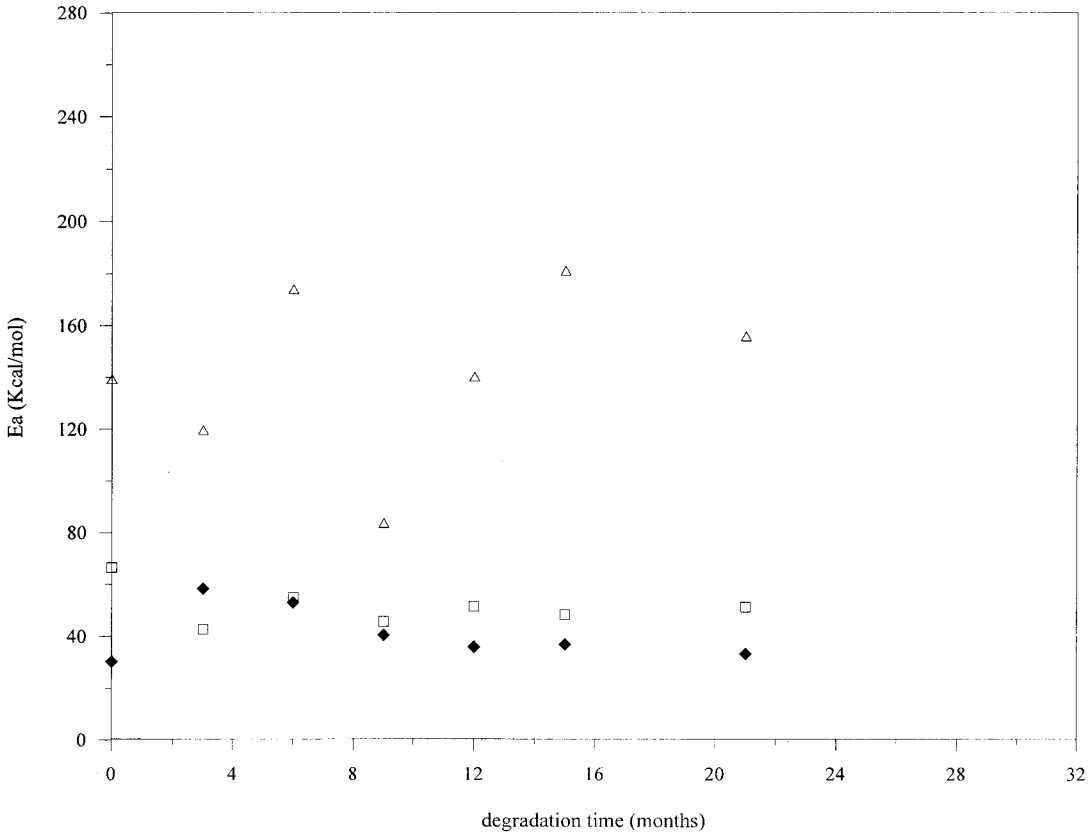

Figure 12 Apparent activation energies E_α of the (□) β, (△) α_I, and (◆) α_{II} relaxations of sample D as a function of the degradation time.

CONCLUSIONS

Due to the degradation process, the HDPE/PP blend and the PP matrix become more brittle, as shown by the increase of the storage modulus E' regardless of the additive used.

The degradation process affects only slightly the amorphous phase of the polymers, as demonstrated by the small changes produced in the γ relaxation.

The analysis of the relaxation spectra shows that the β relaxation is the most sensitive to the degradation process, becoming more prominent as the degradation takes place. Degradation seems to start therefore in the crystalline–amorphous interface.

Although the oxygen is usually insoluble in the crystalline phase and degradation cannot be expected to be initiated in this phase, changes occurring in the amorphous–crystalline interface due to the degradation process affects significantly the crystalline phase. The apparent activation energies of both the α_I and α_{II} relaxations exhibit marked changes. The greatest changes observed for the α_I relaxation indicate that thinner crystallites are more affected by the degradation process than the thicker ones.

On the other hand, the mechanical results correlate well with the calorimetric measurements. The α_{II} relaxation and the crystalline content follow a parallel evolution, confirming the development of the degradation process in two stages with different time scales depending on the additive used.

It can thus be concluded that the analysis of the dynamic-mechanical relaxation spectra may be a useful tool for the study of the degradation process. Together with the analysis of the morphological changes, it can help elucidate the degradation mechanism of polymers.

REFERENCES

1. Griffin, G. J. L. Chemistry and Technology of Biodegradable Polymers; Chapman & Hill, 1994.

2. Albertsson, A. C.; Andersson, S. O.; Karlsson, S. Polym Degrad Stabil 1987, 18, 73–87
3. Goheen, S. M.; Wool, R. P. J Appl Polym Sci 1991, 42, 2691–2701.
4. Greizerstein, H. B.; Syracuse, J. A.; Kostyniak, P. J. Polym Degrad Stabil 1993, 39, 251–259.
5. Vikman, M.; Itävaara, M.; Poutanen, K. JMS-Pure Appl Chem 1995, A32(4), 863–866.
6. Bastioli, C. Polym Degrad Stability 1998, 59, 263–272.
7. Albertsson, A. C.; Barenstedt, C.; Karlsson, S. J Appl Polym Sci 1994, 51, 1097–1105.
8. Karlsson, S.; Hakkarainen, M.; Albertsson, A. C. Macromolecules 1997, 30, 7721–7728.
9. Teh, J. W.; Rudin, A.; Keung, J. C. Adv Polymer Technol 1994. 13(1), 1–23.
10. Martuscelli, E.; Palumbo, R.; Kryszewski, M. Polymer Blends. Processing, Morphology, and Properties; Plenum Press: New York, 1980.
11. Lincoln Hawkins, W. Polymers Properties and Applications, Vol. 8: Polymer Degradation and Stabilization; Springer-Verlag: Berlin, 1984.
12. Wunderlich, B. Macromolecular Physics; Academic Press: New York, 1973.
13. Contat-Rodrigo, L.; Ribes-Greus, A. J Non-Crystalline Solids 1998, 235–237, 670–676.
14. McCrum, N. G.; Reid, B. E.; Williams, G. Anaelastic and Dielectric Effects in Polymeric Solids; Wiley: New York, 1973.
15. Popli, R.; Glotin, M.; Mandelkern, L. J Polym Sci Polym Phys 1987, 22, 407.
16. Ribes-Greus, A.; Díaz-Calleja, R. J Appl Polym Sci 1987, 34, 2819–2828.
17. Charlesworth, J. M. J Materials Sci 1993, 28, 399–404.
18. Sáenz de Juano-Arbona, V.; Ribes-Greus, A.; Díaz-Calleja, R.; Alcaina-Miranda, I.; Del Hierro-Navarro, P.; Sanz-Box, C.; Trijueque-Monge, J. J Non-Crystalline Solids, 1994, 1072,172–174.
19. Albertsson, A.-C.; Barenstedt, C. Karlsson, S. J Environ Polym Degrad 1993, 1(4), 241–245.
20. Albertsson, A.-C.; Karlsson, S. Makromol Chem Macromol Symp 1991, 48/49, 395–402.